Available online at www.sciencedirect.com
ScienceDirect
Journal of Controlled Release 121 (2007) 181–189
journal of controlled release
www.elsevier.com/locate/jconrel

Nano-ferrosponges for controlled drug release

Shang-Hsiu Hu, Ting-Yu Liu, Dean-Mo Liu *, San-Yuan Chen *

Department of Materials Sciences and Engineering, National Chiao Tung University, Hsinchu, 300, Taiwan, ROC

Received 1 March 2007; accepted 5 June 2007
Available online 13 June 2007

Abstract

Magnetic sponge-like hydrogels (ferrosponges) were fabricated by using an in-situ synthesis of magnetic nanoparticles (MNPs) in the presence of various concentrations of gelatin. The resulting ferrosponges show an interconnected nanopore structure which serves as a reservoir to accommodate therapeutic drugs and the nanoporous networks demonstrate magnetic sensitive behavior under the application of magnetic field. The ferrosponges showed high swelling ratios, together with excellent elasticity and hydrophilicity, allow them to response rapidly to an external magnetic stimulation for fast and repeatable swelling-deswelling (or expansion–contractile) operations. The ferrosponges with lower gelatin concentration exhibited good performance on magnetification. Furthermore, drug release from the ferrosponges is relatively magnetic-sensitive and is dominated by its magnetism and associated interaction between the magnetic nanoparticle and the gelatin matrix under an external magnetic field. Higher MNPs concentration in the ferrosponges exhibited higher degree of magnetic sensitive which is due to stronger interparticle forces. By taking these peculiar magnetic sensitive behaviors of the ferrosponges, a novel drug delivery system can be designed for medical uses.

Keywords: Magnetic; Smart; Nanoparticles; Sponge; Controlled drug release

1. Introduction

Environmental sensitive hydrogels (smart hydrogels) with controlled drug release have been received great attention in the field of medicine, pharmaceutics, and biomaterials science. These hydrogels provides advantages over conventional therapeutic dosage forms by having higher delivery efficiency, site-specific delivery, controlled dose, and elimination or reduction of harmful side effects to the patients. By these wide advantages of the hydrogels, a number of researches have been successfully proposed to integrate active drug molecules and host materials, where to manipulate drug release desirably. For example, through conventional bolus injection, drug concentrations at site of therapeutic actions were only a portion of the treatment period in the therapeutic window [1]. By contrast, drug delivery from the controlled polymeric systems could maintain drug concentrations within the therapeutic window for prolonged time.

Such smart hydrogels possess such ‘sensing’ properties which allow to change in swelling behaviors, permeability, and elasticity upon only minute alternations in the environmental conditions. Many physical and chemical stimuli have been applied to induce various responses in response to change in temperature [2–5], pH [6,7], glucose [8], electric field [9,10] and magnetic field [11], for the smart hydrogels [12] which administer drug release considerably and can be potentially used in extended field. So far, many kinds of magnetic sensitive hydrogels (ferrogels) have been developed and studied with regard to biomedical materials. These hydrogels were usually prepared by introducing magnetic nanoparticles into a polymer matrix, and a macroscopic change in the shapes of the resulting ferrogels in response to external magnetic stimuli can be easily manipulated, which permit these ferrogels to be employed as muscle-like soft linear actuators and drug delivery systems [13–15]. For example, magnetic-field-sensitive gelatin microspheres were reported for pulsed release of insulin via an oscillating magnetic field [16] and the release rate of insulin in the alginate microspheres with magnetic particles is much faster than that in absence of an external magnetic field. Although magnetic nanoparticles (MNPs) were widely used for magnetic resonance contrast enhancement, tissue repair, immunoassay, hyperthermia, drug targeting and delivery and in cell separation [17,18], to the best of our knowledge, there has been little investigation on drug delivery

* Corresponding authors. Tel.: +886 3 5712121x31818; fax: +886 3 5725490.
E-mail address: sanyuanchen@mail.nctu.edu.tw (S.-Y. Chen).

0168-3659/$ - see front matter © 2007 Elsevier B.V. All rights reserved.
doi:10.1016/j.jconrel.2007.06.002

under a direct current (DC) magnetic field through the use of magnetic nanoparticles in the ferrogels. Drug delivery from the magnetic sensitive ferrogels can be triggered by a non-contact force (an external magnetic field), which is superior to the traditional stimuli response polymers, such as pH or temperature sensitive polymer. By this concept, a Magnetic Targeted Carriers (MTCs) has been designed which could adsorb pharmaceutical agents through application of an externally magnetic field for site-specific targeting and sustained release of drugs [19]. In addition, according to our previous study, it was demonstrated that a direct current (DC) magnetic field can be used to manipulate the drug release behaviors from a smart magnetic hydrogel through an on-off switch of a magnetic field [20].

However, the drawbacks still exist to use the traditional hydrogels such as thermosensitive or pH-sensitive hydrogels for drug delivery systems. For instance, in some conditions, it is hard for those hydrogels to trigger highly efficiently drug release with a subtle change in the surrounding environments. In the meantime, traditional hydrogels are frequently suffering from fatigue deterioration under repeated operation. On the contrary, magnetic force is a non-contact force which can be used to control drug release of magnetic sensitive gels under the magnetic field [16]. In order to enhance the sensitivity of the hydrogels, Zhang et al. reported that macroporous temperature-sensitive hydrogels exhibited a tremendously faster response to the external temperature changes due to their unique macroporous structures [2,21]. In addition, pHEMA sponges were developed to achieve rapid and reliable delivery of bioactive substances for long-term implantable drug delivery devices [22], and plasmid DNA with a sustained release from polymeric scaffolds was investigated for tissue regeneration [23]. Therefore, in this work, a magnetic-sensitive sponge hydrogels (ferrosponges) was developed in this study to overcome those above-mentioned problems. First, applying a "non-contact" external magnetic field to manipulate the drug release is more robustic. Second, the porous structures (sponge) can improve the magnetic sensitivity because the magnetic nanoparticles are localized in a higher concentrate within thin polymeric walls (i.e., sponge's walls) than those spreading over the entire volume of the bulk or non-porous form. The resulting ferrosponge is able to absorb a large amount of water and shows fast recovery property. Furthermore, magnetic sensitive walls of ferrosponges constructed by MNPs can effectively reduce their wall permeability and decrease the drug release via a given magnetic field as shown in Fig. 1. For this purpose, a magnetic sponge hydrogel composed of a biocompatible gelatin and magnetic nanoparticles (MNPs) is investigated in terms of the concentrations of magnetic nanoparticle and gelatin. The drug release behavior from this ferrosponge in response to a magnetic field is investigated.

2. Materials and methods

2.1. Chemicals and regents

The commercially available gelatin from bovine skin (type A, ~300 bloom), 1-Ethyl-3-(3-Dimethylaminopropyl) Carbodiimide Hydrochloride (EDC) and model drug vitamin B12 were purchased from Sigma Chemical Co. Iron (II) chloride ($FeCl_2$) and Iron (III) Chloride ($FeCl_3$) were obtained from Fluka and Riedel-deHaen, respectively, and used as received. Ammonia hydroxide (NH_4OH) in the form of 33% water solution was obtained from Riedel-deHaen. Phosphate buffered saline (PBS) was purched form Ultra Biotechnology Corporation.

2.2. Preparation of the ferrosponges

Magnetic sponge hydrogels (ferrosponges) were fabricated by in-situ co-precipitation process, and iron oxide nanoparticles were deposited directly in the gelatin hydrogel. Briefly, gelatin was dissolved in the D.I. water for 2 h at 40 °C. After gelatin was fully dissolved in the solution, appropriate amount of $FeCl_2$ and $FeCl_3$ was added to the gelatin solution to form the hybrid sols. (The molar ratio of $FeCl_2/FeCl_3$ was kept constant at 1:2, and the reagents used for synthesis was showed in Table 1.) When completely dissolved, the hybrid sols were rapid cooled to 4 °C to gel the gelatin which was then immersed in a water solution of NH_4OH to start the iron oxide formation process. Immediately, the gels became black, indicating that the iron oxide nanoparticles have been formed in the system. After the

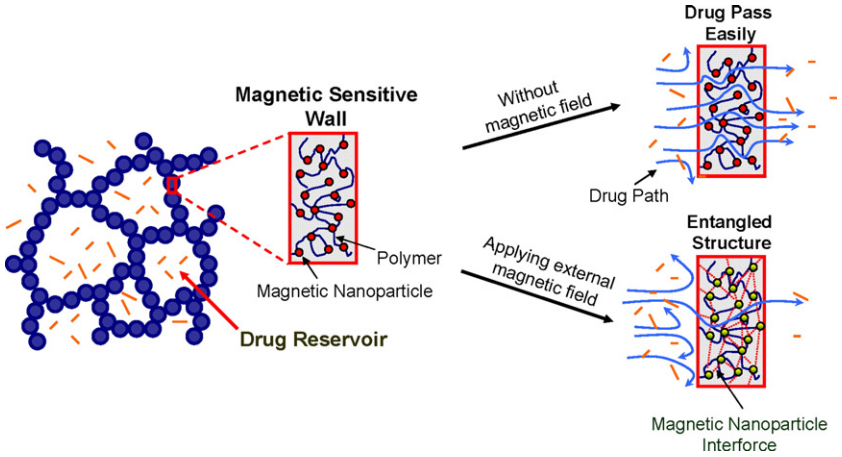

Fig. 1. Schematic drawing of drug release from the magnetic-sensitive ferrosponges with and without applying external magnetic field.

Table 1
Reagents used for the synthesis of ferrosponges

System	Sample	Gelatin (g)	$FeCl_2$ (g)	$FeCl_3$ (g)	water (mL)	S %[a]	MNPs[b] (wt.%)
5G series	5G–1F	5	1	2.7	100	10.1	3.7
	5G–3F	5	3	7.1	100	8.1	6.5
	5G–5F	5	5	13.5	100	6.1	9.4
15G series	15G–1F	15	1	2.7	100	9.4	2.7
	15G–3F	15	3	7.1	100	7.7	5.3
	15G–5F	15	5	13.5	100	6.7	7.1

[a] S%: Swelling ratio=(weight of wet ferrosponge)/(Weight of dried ferrosponge).
[b] MNPs (wt.%): The weight fraction of magnetic nanoparticles(MNPs) measured by TGA.

in-situ co-precipitation of iron oxide nanoparticles, the ferrosponge were washed by D.I. water for several times to remove un-reacted NH_4OH solution, and then the ferrosponge were subsequently kept in the freezing baths maintained at −80 °C for 1 day and finally lyophilized in a freeze-dryer for 3 days. Finally, the macroporous structures were formed and cured by 1-ethyl-3-[3-(dimethylammino) propyl]carbodiimide (EDC) in the 9:1 acetone:water solution at 4 °C.

2.3. Characteristics

The Raman spectra were obtained using a backscattering geometry. The 632 nm of a He-Ne laser was focused through an Olympus microscope with a 100× lens to give a spot size of 1 μm. The spectra was obtained using a 60 s acquisition time and averaged over 3 accumulations. X-ray diffractometer(XRD, M18XHF, Mac Science, Tokyo, Japan) was used to identify the crystallographic phase of ferrosponges, at a scanning rate of 6° 2θ per min over a range of 2θ form 10° to 70°. Additionally, the magnetization of the ferrosponges was measured with a vibrating-sample magnetometer (VSM, Oxford) at 298 K and ±0.6 Tesla applied magnetic field. The relative amount of the magnetic nanoparticles associated with the gelatin was determined using thermo-gravimetric analysis, TGA (Perkin Elmer). Samples were dried in a vacuum for ~48 h and analyzed in the platinum plate at a heating rate of 10 °C/min under nitrogen atmosphere. The porous structure of ferrosponges and morphologies of magnetic nanoparticles were examined using field emission scanning electron microscopy (FE-SEM, JEOL-6500, Japan). After thermally removing gelatin from ferrosponges, pore sizes of nano-structural iron oxide nanoparticles were determined by BET analysis. By measurement of N_2 gas absorption isotherms at 77 K, the pore size were calculated following the approach by Barrett, Joyner, and Halenda (BJH).

2.4. Release kinetics of the ferrosponges

Vitamin B12 (Sigma, V-2876) was used as model drug in this composite system because it is a water-soluble agent with low molecular weight, and its colorful nature allows a direct visual observation during the test, and almost shows negligible interaction with gelatin or MNPs. Before loading drug, the ferrogels were immersed and washed by D.I. water to remove un-reacted iron salts. In the preparation of the drug-loaded ferrosponges, the ferrosponges were soaked in 1% vitamin B12 of 50 ml PBS solution for drug loading. Before conducting the drug release test, the drug-loaded ferrosponges were first washed to remove the drug on the surface. The drug release behavior of the ferrosponges was measured using 50 ml phosphate buffered saline per sponge cube (pH 7.4). The drug contents of the ferrospnges were measured after the drug was entirely released. UV–Visible spectroscopy (Agelent 8453) was used for characterization of absorption peak at 361 nm to quantitatively determine the vitamin B12.

To investigate the diffusion mechanism of the drug molecules in the gel, the drug released data were characterized using Eq. (1): [24]

$$\frac{M_t}{M} = kt^n \tag{1}$$

where M_t is the mass of drug released at time t, M is the mass released at time infinity, and M_t/M is the fractional mass of released drug; k is a rate constant, and n is a characteristic exponent related to the mode of transport of the drug molecules. By taking logarithm on both sides of Eq. (1), Eq. (2) can be used to calculate the diffusion parameters (i.e., n and k) for $M_t/M<0.6$.

$$\ln\left(\frac{M_t}{M}\right) = n\ln t + \ln k \tag{2}$$

The cumulative concentrations of released drug at time t and at the end of the experiment (to approximate the infinite time) were used to calculate M_t/M.

A direct-current (DC) magnetic field (MF) with 0.04 Tesla was applied to control the drug release profiles from the ferrosponges. The release of the drug from the ferrosponges was measured at a controlled temperature of 37±0.1 °C in a flow-through cell with 40 ml phosphate buffered solution. The drug release behavior of the ferrosponges was characterized with the continuously applied magnetic field. Furthermore, the external magnetic fields switched alternatively between "on" (MF ON) and "off" (MF OFF) mode in a 30-minute period was applied for several cycles in order to investigate the anti-fatigue property of the ferrosponges.

3. Results and discussion

3.1. Synthesis of ferrosponges

Magnetic-sensitive ferrosponges composed of gelatin and magnetic nanoparticles (MNPs) were prepared through an in-situ co-precipitation process. The traditional method of preparing iron oxide nanoparticles usually used the chemical co-precipitation of iron salts in the alkaline medium:

$$Fe^{2+} + 2Fe^{3+} + 8OH^- \rightleftharpoons Fe(OH)_2 + 2Fe(OH)_3 \rightarrow Fe_3O_4 + H_2O$$

However, the iron oxide nanoparticles formed by using this traditional method aggregated easily [25]. To prevent aggregation, the gelatin and iron salts were mixed in advance to become a homogeneous mixture in which iron cation and the carboxylic

acid groups of polymer allow to form a homogeneous complex structure in the solution [25]. While the ammonia solution was added, the iron oxide nanoparticles were directly formed in the presence of the gelatin, resulting in a sponge-like structure after lyophilizing. The ferrosponges shown in Fig. 2 exhibited a three-dimensional porous structure with macroporous and an anastomosing network of gelatin matrix. The mean pore size shown in Fig. 2(A) for the 5 wt.% gelatin matrix of ferrosponges was microscopically measured to be 100±23 μm, which was larger than that (50±24 μm) for the 15 wt.% gelatin matrix of ferrosponges, Fig. 2(B). It was found that the morphology and pore size of the ferrosponges seemed to be greatly dependent upon the gelatin matrix rather than the amounts of MNPs. The macropores of the ferrosponges appeared to be well-arranged, which displayed membrane-like wall structure. The magnified image in the 2(B) showed the surface morphology of the ferrosponge, where a rougher surface than that of traditional sponges was observed in the ferrosonges, which is due to the presence of the MNPs in the ferrosponges.

3.2. Characterization of magnetic-sensitive ferrosponges

3.2.1. Crystalline phase identification

X-ray diffraction (XRD) analysis showed that the crystalline phases of iron oxide in the ferrosponges are γ-Fe_2O_3 (maghemite)

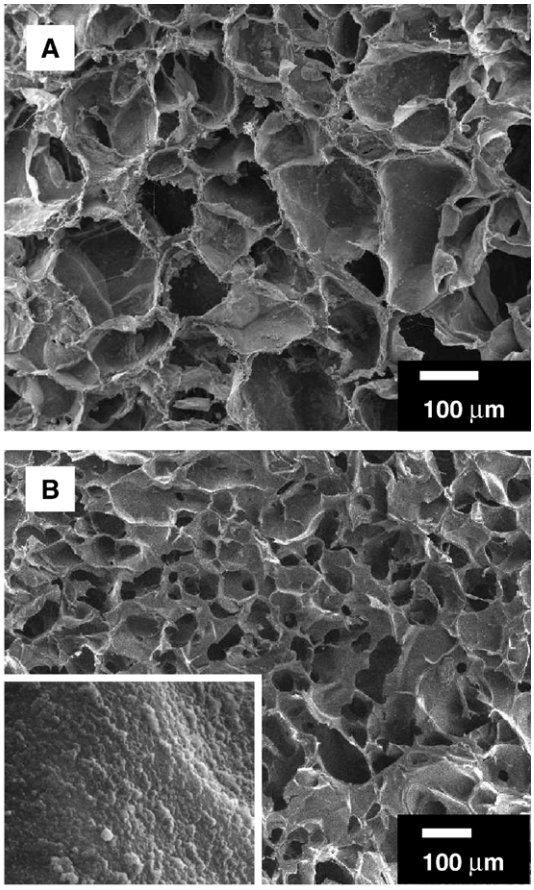

Fig. 2. SEM images of the ferrosponges for 5 wt.% (A) and 15 wt.% (B) gelatin concentrations.

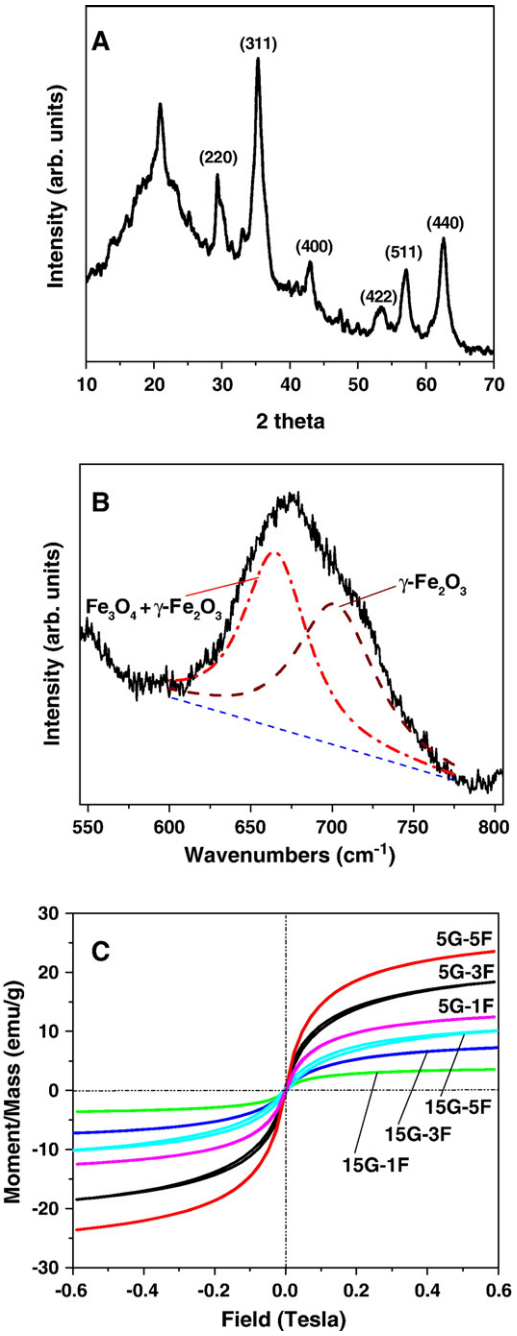

Fig. 3. (A) XRD and (B) Raman spectra of the ferrosponges. (C) Vibrating sample magnetometry measurements for the ferrosponges with various contents of iron oxide nanoparticles.

or Fe_3O_4 (magnetite), Fig. 3(A). However, it is very difficult to distinguish Fe_3O_4 from γ-Fe_2O_3 because these two phases exhibited similar XRD patterns (according to Fe_3O_4 (JCPDS [85-1436]) and γ-Fe_2O_3 (JCPDS [04-0755])) [26]. In addition to the diffraction peaks of iron oxide, one more peak at $2\theta \sim 21°$ was observed and can be identified as the semi-crystalline gelatin. Furthermore, the diffraction data were also used to measure the primary particle size according to Scherrer analysis for diffraction peak widths of (311) peak, wherein the (311) peak is common to both magnetite and maghemite phases. The primary particle size

of iron oxide in the ferrosponges was estimated ranging from 8 to 12 nm.

Raman spectroscopy is potentially more useful than the X-ray diffraction techniques in distinguishing γ-Fe_2O_3 from Fe_3O_4 and was used to track subtle structural differences between the vibration frequencies of γ-Fe_2O_3 and Fe_3O_4 [27]. Fig. 3(B) shows that, although the iron oxide nanoparticles were surrounded with gelatin, a significant difference between these phases can be recognized from the Raman spectrum. The 665 cm^{-1} band, assigned to the characteristic band of Fe_3O_4, observed in the Raman spectra displays a symmetrical peak and is attributed to the vibration modes consisting of stretching of oxygen atoms along Fe-O bonds. On the other hand, the characteristic peaks for γ-Fe_2O_3 present at 721 cm^{-1} and a weaker band at 667 cm^{-1} [26]. Both evidences support the ferrosponges consisting of γ-Fe_2O_3 and Fe_3O_4 phases.

As the result shown in Table 1, the content of iron oxide nanoparticles in the sample 5G–5F could reach 9.4% measured by TGA. It was observed that the amount of the iron oxide nanoparticles were related to the starting concentration of iron salts. Generally, it was thought that the amount of iron oxide nanoparticles were proportional to the concentration of iron salts, albeit not in a direct proportional correlation, they do exist a linear relationship. This is due to the fact that the inorganic nanoparticles directly formed in the polymer matrix could be hindered by polymer-particle interactions [25,28]. Therefore, the amount of iron oxide nanoparticles developed in sample 5G–5F was lower by five times than that in sample 5G–1F.

3.2.2. Magnetic property

The magnetic properties of the ferrosponges with various iron oxide contents were studied with VSM at ambient temperature, with the magnetic field sweeping from −0.6 to +0.6 Tesla. As shown in Fig. 3(C), the magnetization-magnetic field curves for all the ferrosponges show similar shape with negligible hysteresis. This indicates that these ferrosponges exhibit super-paramagnetic characteristics but with different saturation magnetization (Ms). The sample 5G–5F displayed the largest Ms of 23.6 emu/g, and it was observed that the Ms decreased with the decrease of iron oxide. The saturation magnetization (Ms) of the ferrosponges was also dependent on the inorganic/organic ratios, as summarized in Table 1. However, although the weight fractions of MNPs in the 15G series are slightly lower than those in the 5G series, the inorganic/organic ratios of 15G series are much lower as compared with 5G series. Correspondingly, the Ms for 15G series was lower than that for 5G series. The correlation of the Ms with the magnetic sensitive behaviors of these ferrosponges will be discussed in forthcoming analysis.

3.2.3. Nanostructural analysis

In order to examine the microstructure and morphology of the resulting nanoparticulate network structure, the gelatin was intentionally removed thermally while a porous structure made of the magnetic nanoparticles remained intact.

The pores in the magnetic solid network structure are characterized as two categories; one with a size ranging from 100–200 nm, as a macroporosity, located between the walls or struts, and the one inside the walls or struts has a size of only a few nanometers, as a mesoporosity. Such a mesoporosity is formed due partly to thermal removal of the gelatin between the nanoparticles, and in part, as an interparticle voids developed upon in-situ synthesis, as shown in Fig. 4. In comparison with 5G–5F and 15G–5F, in Fig. 4(A) and 4(B), respectively, sample 5G–5F exhibited looser structure than that of the sample 15G–5F, having a denser structure when the gelatin was completely burned off. However, it seems no considerable difference between the mesosporosity of these two samples. Therefore, it can be concluded that the concentration of gelatin used to synthesize the

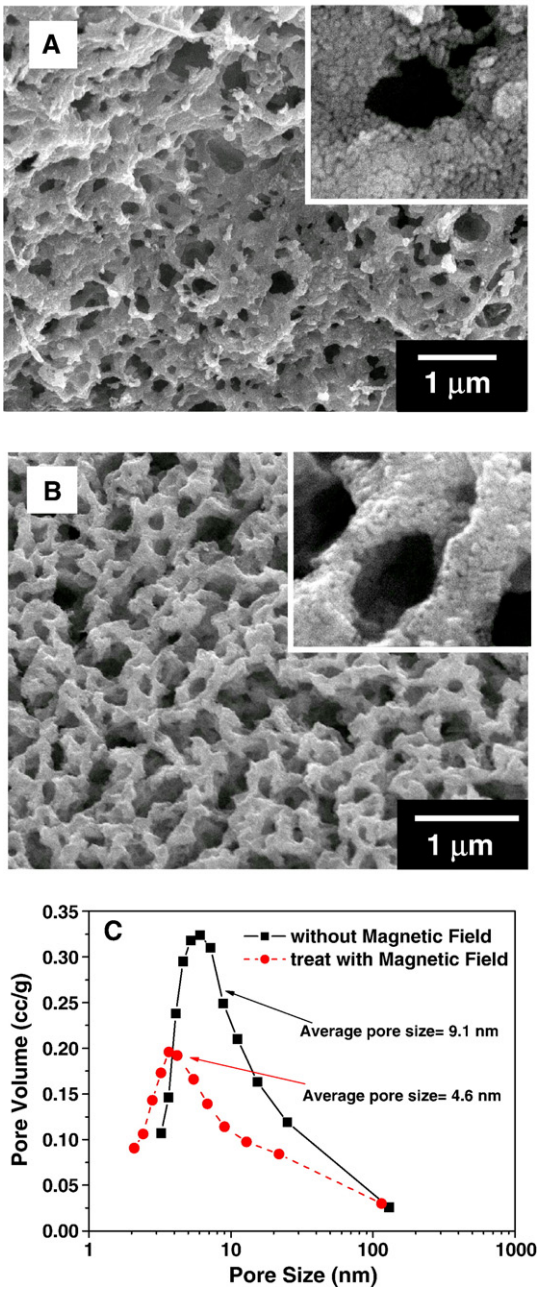

Fig. 4. SEM images of iron oxide nanoparticles structure of the sponges obtained by thermally removing gelatin matrix for the ferrosponges with original 5G–5F (A) and 15G–5F(B) compositions, and associated with the pore size distribution of the ferrosponges treated with and without magnetic field (C).

ferrosponges affects strongly the macroporosity of the sponge but negligibly for mesoporosity development. High resolution SEM images of 5G–5F and 15G–5F were presented in Fig. 4(A) and (B), respectively. The iron oxide nanoparticles were clearly observed and exhibited a spherical shape with average particle size about 10 nm, which is relatively closed to the size calculated by Scherr's equation. Such a nanometric scale of the magnetic particles allows the achievement of super-paramegnetization upon magnetic stimulation and this is evidenced in Fig. 3(C) where little or no hysteresis behavior was detected. The pore size distribution of iron oxide nanoparticles exhibited in Fig. 4(C) demonstrated that there were numerous nanopores within the magnetic nanostructures. The mean pore diameter was 9.1 nm, and the pore size distribution ranged from 3 nm to 30 nm, which may affect the diffusion rate of the B12 molecules. It is also conceivable that a manipulation of these nanopores by a magnetic force can be effectively used for a control release of drug. The sizes of mesopores after treating with magnetic field decreased considerably (Fig. 4C) in pore volume and pore size, to an average size of 4.6 nm, indicating a result of re-arrangement of the magnetic nanoparticles to form more compact, rigid structure. Although the change in the pore size is detected from the magnetic nanoparticle network, this can also be translated as shrinkage in the pore size in the ferrosponge upon applying a magnetic field. The variation of the mesopores in the ferrosponges under magnetic stimulation is able to act as a diffusion regulator for control release of drug molecules.

3.3. Drug release behaviors of ferrosponges

Therefore, along the line of magnetic manipulation, drug (vitamin B12) release profiles from the ferrosponges were expected and demonstrated in Fig. 5. Initial burst release was observed from the ferrosponges in the first 60 min and the amounts of drug release from the ferrosponges were almost equal for all the ferrosponges. Although the ferrosponges had been washed before the releasing test, the initial burst was believed to result from the outermost layer of the ferrosponges. After the initial burst, the ferrosponges showed different release rates, from 60 to 250 min, according to the concentration of the nanoparticles. Typically, pure gelatin sponge showed a faster drug release rate than that of the nanoparticle-containing ferrosponges. According to our previous studies, it demonstrated that a strong interaction exists between iron oxide nanoparticles and polymer side chains in the composite [29]. In addition, Hongbin et al. also reported that the inorganic nanoparticles restricted relaxation behavior in the nanocomposites because of the polymer–nanoparticle interactions [30].

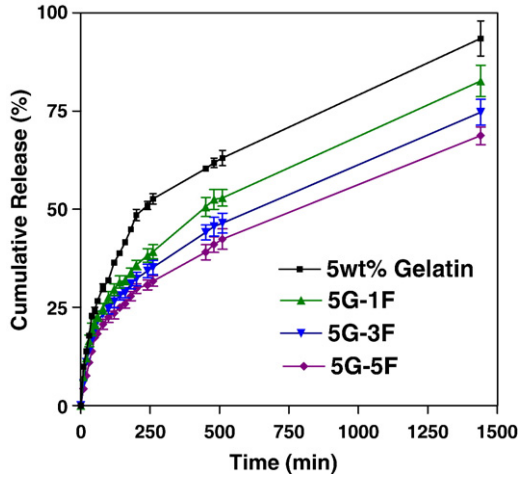

Fig. 5. The drug release profiles of 5G series of the ferrosponges.

When these strong interactions were developed in the ferrosponges, the drug-release behavior can be affected and restricted via molecular relaxation. The drug molecules released from a nanocomposite can be blocked by the nanoparticles, acting as a physical barrier for drug diffusion. In the meantime, the presence of numerous nanoparticles along the path of drug diffusion gives rise to a considerable increase in the mean free path for drug diffusion. Therefore, the drug released from the ferrosponges showing a lower rate than that from pure gelatin sponges. A near-linear drug release profile was later developed after a time period greater than 250 min for all the samples, irrespective of the presence of nanoparticles, suggesting the release of the drug is reaching a state-steady diffusion. Again, the higher concentration of the nanoparticles in the ferrosponges, the lower amount of the drug was released in this linear-kinetic region. This indicates the rate of drug release being considerably retarded by those nanometric physical barriers in the matrix, but the release profiles for all the ferrosponges appeared following a similar (near)zero-order kinetics according to Fig. 5.

3.4. Magnetically controlled drug release

Fig. 6(A) shows the release profiles of vitamin B12 from the ferrosponges under "on" and "off" operations of an external magnetic field (MF) at 37 °C. The amount of drug that released under "on" mode was relatively low; about 25%, compared to that operated under "off" mode, 40%, over a time span of 360 min. This finding strongly indicates that the applied magnetic field effectively retarded drug release from the ferrrosponge of 5G–5F composition by as large as 60%. More specifically, the drug release profile is considerably changed even from the very beginning of release when the ferrosponge was subjecting to a given MF. The release kinetic showed a parabolic profile from the beginning to about 120 min, after then, a linear profile of drug release followed till the end of the release test.

By taking Eq. (2), a kinetic analysis of drug release from the 5G–5F ferrosponge can be obtained, as shown in Fig. 6(B), where a two-stage release kinetics for the ferrosponge is displayed, with and without the presence of the magnetic field. Both exponent constant, n and rate constant, k, are estimated. For the first-stage release kinetics, the exponent constant is in a range of 0.5–0.6, indicating a typical Fickian diffusion mode, suggesting diffusion rate is dominating the drug release over relaxation rate in the ferrosponges. However, the exponent constants are apparently decreased to a range of 0.28–0.36 at the second stage of the profile, indicating the diffusion at the

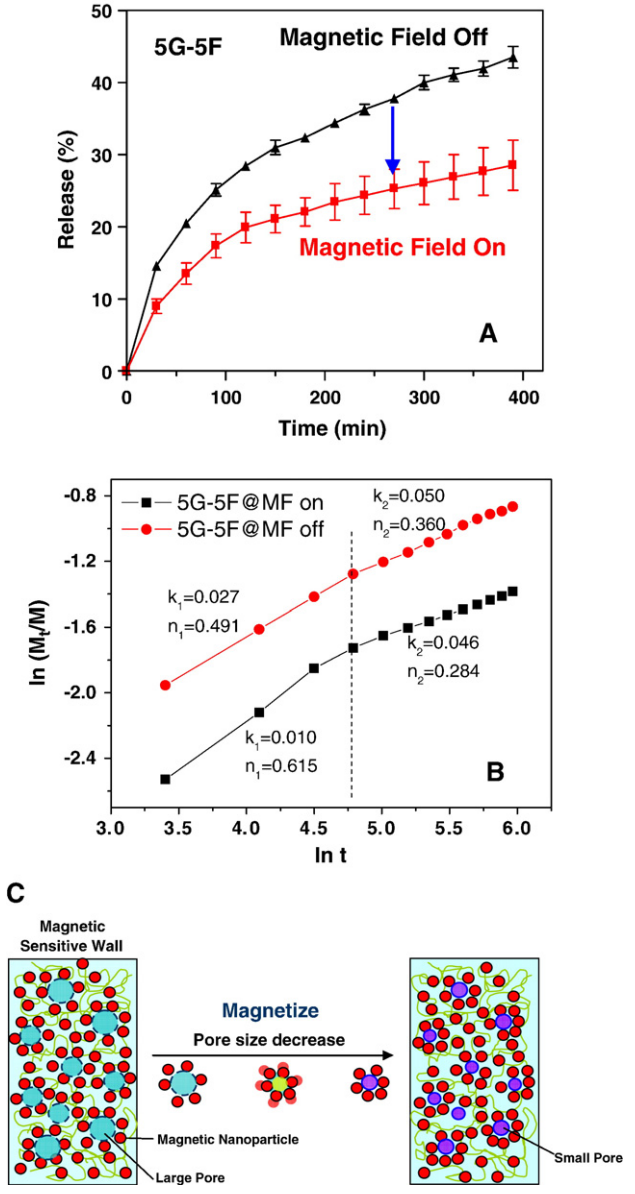

Fig. 6. (A)The drug release profiles with and without applying magnetic field ("MF on" and "MF off", respectively.) for 5G–5F ferrosponge. (B) A plot of ln (M_t/M) versus ln (t) of 5G–5F showed a two-step relationship for calculating the values of k and n, and the corresponding schematic drawing of the shrinkage of the mesopores in the ferrosponges (C) while a magnetic field was applying.

second stage being heavily retarded and it turned out to be more pronounced under magnetic field, having the lowest n value. It is suggestive of an enhanced retardation for drug molecules to diffuse through the ferrosponges under magnetic field. However, since it is hard to give a precise measurement of the pore sizes in the ferrosponges, so the gelatin was removed from the ferrosponges in order to facilitate the estimate of the pore sizes within the nanoparticle network instead. The relative change in pore size and distribution for the nanoparticle network under MF operation do show a significant evidence of such a variation, as shown in Fig. 4(C), and it is believed to translate directly to the condition of actual nano-ferrosponges. The reduction in pore size and a corresponding shift in pore size distribution to smaller pore region under magnetic field of the magnetic particulate network of the ferrosponge provide evidence of a diffusion barrier for drug movement in the magnetized ferrosponges. Similar release kinetic parameters can be found for the ferrosponges of different compositions, and the constants are listed in Table 2. The rate constant, k, for all the ferrosponges at both release stages has apparently lower k value in the presence of magnetic field, than those without the field. This change in release kinetic is believed to be a change in the distribution of the nanoparticles when an MF is applied. The first-stage release profile (kinetically similar to that observed for the ferrosponge under no MF) appeared to be less magnetically controllable because it corresponds to the drug release from macroporosity of the magnetic particle networks which is corresponding to a released amount of 19%. The re-alignment of the magnetic nanoparticles, (or nano-magnets) within the ferrosponges has little effect on blocking drug diffusion from those macroporosity. Nevertheless, the drug is highly regulated from mesoporosity of the ferrosponges, as a result of aggregation of those nano-magnets in the ferrosponges. The diffusion path was highly confined, resulting in a much slower diffusion of the drug molecules from the ferrosponge. Table 2 show that the k values of 5G–1F under "MF on" and "MF off" are similar, but the k values for 5G–5F obviously vary and present difference under "MF on" and "MF off" because the k values are strongly influenced by the amounts of magnetic nanoparticles in the ferrosponges. A lower value of the rate constants, i.e., k_1 and k_2, indicating a lower frequency of molecular activity, prevailed in the magnetized ferrosponges than those without magnetization for both stages of release profile provides direct evidence of the magnetically-induced inhibition effect on molecular diffusion.

The mechanism of drug release profiles from the ferrosponges can then be elucidated as schematically illustrated in Fig. 6(C). The walls between the macropores in the magnetic particle network of the ferrosponge possess large amounts of mesopores, in which drug release is solely dominated by molecular diffusion through the mesopores to environment. By magnetizing the iron oxide nanoparticles in the walls, the mesopore size decreased considerably, which restricted more effectively the diffusion of the drug molecules. Consequently, the drug release rates decreased immediately while applying an external magnetic field. The interaction between magnetic particles has been demonstrated to occur under an external

Table 2
The k and n values of ferrosponges under the modes of magnetic on(MF on) and off(MF off)

		5G–1F	5G–3F	5G–5F	15G–1F	15G–3F	15G–5F
$k1$	MF off	0.037	0.033	0.027	0.020	0.018	0.019
	MF on	0.030	0.020	0.010	0.014	0.012	0.011
$k2$	MF off	0.066	0.055	0.050	0.036	0.023	0.023
	MF on	0.057	0.053	0.046	0.032	0.019	0.019
$n1$	MF off	0.460	0.475	0.491	0.548	0.563	0.577
	MF on	0.470	0.527	0.615	0.618	0.595	0.590
$n2$	MF off	0.341	0.362	0.360	0.423	0.506	0.516
	MF on	0.334	0.314	0.284	0.377	0.483	0.497

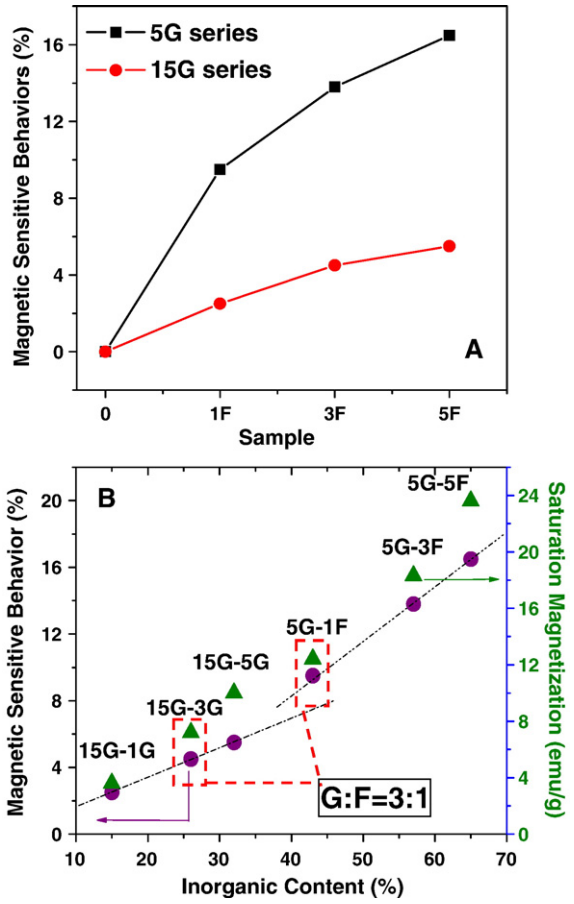

Fig. 7. (A) A comparison of the magnetic-sensitive behaviors of the ferrosponges for both 5G and 15G series compositions. (B) The inorganic/organic ratios of ferrosponges related to the magnetic sensitive behaviors (%) and saturation magnetization (Ms).

magnetic field [31]. For two identical particles with magnetic moment M, interaction energy can be given as follows:

$$E_i \propto \frac{M^2}{r^3}(3\cos\psi_1\cos\psi_2 - \cos\alpha) \quad (3)$$

where r is the distance between two particles, ψ_1 and ψ_2 are the angles between r and two moments, respectively, and α is the angle between the two moments. From Eq. (3), it is clear that the distance between the magnetic nanoparticles (r) is also strongly related to the intensity of interaction energy. The shorter distance between iron oxide nanoparticles displayed stronger interactions and this is one of main reasons for the ferrosponges to demonstrate better magnetic-sensitive behaviors.

3.5. Magnetic-sensitive behavior

The preliminary result demonstrated that the ferrosponges possessed magnetic-sensitive behaviors under an MF. The "Magnetic Sensitive Behavior (%)" was defined as the difference in the amount of cumulative drug release under "MF off" minus that under "MF on". The higher value of the "Behavior" indicates the higher sensitivity of the ferrosponge to a given strength of magnetic field in terms of drug release.

Fig. 7(A) shows the magnetic-sensitive behaviors for the ferrosponges of 5G and 15G compositions. The magnetic-sensitive behavior showed about 4–5 times more pronounced for the 5G compositions than that for the 15G series. It is possible that ferrosponge with 5G compositions possess a better elastic property and at the same time, a stronger interparticle attraction to regulate the relaxation of the gelatin molecules than those of 15G compositions, resulting in the sharply enhanced magnetic-sensitive behaviors. More plausibly, according to a recent study on the concentration effect of the nano-magnets on magnetization of a PVA-based ferrogels [32], it is believed that under the same relative concentration of the nano-magnets, the ferrosponges with higher relative concentration of the gelatin showed lower magnetization, and is evidenced in Fig. 7(B), where the saturation magnetization is increased linearly with increasing nano-magnet concentration and decreased with increasing gelatin concentration. On this base, it realizes that the nano-magnet concentration in the ferrosponges causes a significant variation in magnetic-sensitive behavior. Fig. 7(B) further supports a stronger interparticle attraction force and less rigidity (i.e., the molecular relaxation of the gelatin chains being less restricted) of the 5G ferrosponges. Furthermore, although 5G–1F and 15G–5F possessed the same gelatin-to-Fe_3O_4 ratio (i.e., G/F = 3/1), 5G–1F exhibited more than twice the magnetic sensitive behaviors to that of the 15G–5F composition, because in 5G–1F, the magnetic nanoparticles binding on the looser polymer structure could be migrated easily.

Upon a consecutive on-off operation of the magnetic field to the ferrosponges, an alternative change in drug release can be identified, as shown in Fig. 8. The cumulative drug-release amount decreased with applied magnetic field and increased again while the MF was turned off. This tunable release rate further substantiates the re-arrangement of the magnetic nanoparticles and this further indicates a potential use of this novel ferrosponges for drug delivery applications. With increasing

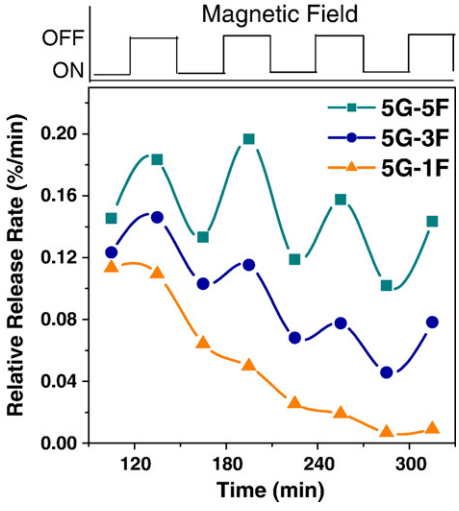

Fig. 8. The relative drug release rates of the ferrosponges under repeated on-off MF operations, showing a fast degradation in the release rate with less MNP concentration, but much improved release behavior with respect to cyclic operation when MNP is increased and seems to be optimized in 5G–5F composition, i.e., indicating an improved anti-fatigue property.

concentration of the nano-magnets, i.e., from 1F to 5F composition, the ability for the ferrosponges to reaching a considerable drug release rate is increased significantly when the ferrosponges to reach a consecutive MF on-off operation. This suggests that the ferrosponges gain sufficient elasticity with the incorporation of critical amount of the nano-magnets, which can be elucidated in the ferrosponge with 5G–5F composition. This also indicates a considerable improvement of the anti-fatigue property of the ferrosponges, compared to neat gelatin matrix, further encouraging the use of the ferrosponges for drug delivery application.

4. Conclusion

Nano-ferrosponges with tunable magnetic sensitive behavior were successfully prepared by an in-situ synthesis of magnetic nanoparticles in the presence of gelatin. Nanopores with size ranging from 2 to 100 nm in diameter can be synthesized within the magnetic nanoparticulate network.The nanopores are then manipulated with a reduced size by externally controlled magnetic field, which allows the resulting ferrosponges suitable for control release of active agents. Release kinetics of a model drug, i.e., vitamin B12, also showed a series of tunable kinetic parameters under magnetization, and this finding allows a slow release of drug molecules achievable for practical uses. Ferrosponge with optimal 5G–5F composition was evaluated, where an optimal "magnetic sensitive behavior" was detected as a result of its stronger Ms and looser polymeric structure. Furthermore, the ferrosponge with 5G–5F composition also illustrated a consdierably improved anti-fatigue property under repeated on-off MF operations for a consecutive drug release control.

References

[1] K.E. Uhrich, S.M. Cannizzaro, R.S. Langer, K.M. Shakesheff, Polymeric systems for controlled drug release, Chemical Reviews 99 (1999) 3181–3198.

[2] X.Z. Zhang, D.Q. Wu, C.C. Chu, Synthesis, characterization and controlled drug release of thermosensitive IPN–PNIPAAm hydrogels, Biomaterials 25 (2004) 3793–3805.

[3] F. Eeckman, A.J. Moës, K. Amighi, Poly(N-isopropylacrylamide) copolymers for constant temperature controlled drug delivery, International Journal of Pharmaceutics 273 (2004) 109–119.

[4] A. Gutowska, J.S. Bark, I.C. Kwon, Y.H. Bae, Y. Cha, S.W. Kim, Squeezing hydrogels for controlled oral drug delivery, Journal of Controlled Release 48 (1997) 141–148.

[5] G.N.C. Chiu, S.A. Abraham, L.M. Ickenstein, R. Ng, G. Karlsson, K. Edwards, E.K. Wasan, M.B. Bally, Encapsulation of doxorubicin into thermosensitive liposomes via complexation with the transition metal manganese, Journal of Controlled Release 104 (2005) 271–288.

[6] T. Etrych, M. Jelínková, B. Říhová, K. Ulbrich, New HPMA copolymers containing doxorubicin bound via pH-sensitive linkage: synthesis and preliminary in vitro and in vivo biological properties, Journal of Controlled Release 73 (2001) 89–102.

[7] S.C. Chen, Y.C. Wu, F.L. Mi, Y.H. Lin, L.C. Yu, H.W. Sung, A novel pH-sensitive hydrogel composed of N,O-carboxymethyl chitosan and alginate cross-linked by genipin for protein drug delivery, Journal of Controlled Release 96 (2004) 285–300.

[8] L.Y. Chu, Y. Li, J.H. Zhu, H.D. Wang, Y.J. Liang, Control of pore size and permeability of a glucose-responsive gating membrane for insulin delivery, Journal of Controlled Release 97 (2004) 43–53.

[9] S. Murdan, Electro-responsive drug delivery from hydrogels, Journal of Controlled Release 92 (2003) 1–17.

[10] K. Sutani, I. Kaetsu, K. Uchida, The synthesis and the electric-responsiveness ofhydrogels entrapping natural polyelectrolyte, Radiation Physics and Chemistry 61 (2001) 49–54.

[11] M. Zrínyi, Intelligent polymer gels controlled by magnetic fields, Colloid Polymer Science 278 (2000) 98–103.

[12] Y. Qiu, K. Park, Environment-sensitive hydrogels for drug delivery, Advanced Drug Delivery Reviews 53 (2001) 321–339.

[13] T. Mitsumata, K. Ikeda, J.P. Gong, Y. Osada, D. Szabó, M. Zrínyi, Magnwtism and compressive modulus of magnetix fluid containing gels, Journal of Applied Physics 85 (1999) 8451–8455.

[14] P.M. Xulu, G. Filipcsei, M. Zrínyi, Preparation and responsive properties of magnetically soft poly(N-isopropylacrylamide) gels, Macromolecules 33 (2000) 1716–1719.

[15] M. Zrínyi, D. Szabó, H.G. Kilian, Kinetics of the shape change of magnetic field sensitive polymer gels, Polymer Gels and Networks 6 (1998) 441–454.

[16] O. Saslawski, C. Weingarten, J.P. Benoit, P. Couvreur, Magnetically responsive microspheres for the pulsed delivery of insulin, Life Science 42 (1988) 1521–1528.

[17] A.K. Gupta, M. Gupta, Synthesis and surface engineering of iron oxide nanoparticles for biomedical applications, Biomaterials 26 (2005) 3995–4021.

[18] T. Neuberger, B. Schöpf, H. Hofmann, M. Hofmann, B.V. Rechenberg, Superparamagnetic nanoparticles for biomedical applications: Possibilities and limitations of a new drug delivery system, Journal of Magnetism and Magnetic Materials 293 (2005) 483–496.

[19] J. Fricker, F. Writer, Drugs with a magnetic attraction to tumours, Drug Discovery Today 6 (2001) 387–389.

[20] T.Y. Liu, S.H. Hu, K.H. Liu, D.M. Liu, S.Y. Chen, Preparation and characterization of smart magnetic hydrogels and its use for drug release, Journal of Magnetism and Magnetic Materials 304 (2006) e397–e399.

[21] X.Z. Zhang, Y.Y. Yang, T.S. Chung, K.X. Ma, Preparation and characterization of fast response macroporous poly(N-isopropylacrylamide) hydrogels, Langmuir 17 (2001) 6094–6099.

[22] T.D. Dziubla, M.C. Torjman, J.I. Joseph, M. Murphy-Tatum, A.M. Lowman, Evaluation of porous networks of poly(2-hydroxyethyl methacrylate) as interfacial drug delivery devices, Biomaterials 22 (2001) 2893–2899.

[23] H. Storrie, D.J. Mooney, Sustained delivery of plasmid DNA from polymeric scaffolds for tissue engineering, Advanced Drug Delivery Reviews 58 (2006) 500–514.

[24] P.L. Ritger, N.A. Peppas, A simple equation for description of solute release II. Fickian and anomalous release from swellable devices, Journal of Controlled Release 5 (1987) 37–42.

[25] C.L. Lin, C.F. Lee, W.Y. Chiu, Preparation and properties of poly(acrylic acid) oligomer stabilized superparamagnetic ferrofluid, Journal of Colloid and Interface Science 291 (2005) 411–420.

[26] J.W. Long, M.S. Logan, C.P. Rhodes, E.E. Carpenter, R.M. Stroud, D.R. Rolison, Nanocrystalline iron oxide aerogels as mesoporous magnetic architectures, Journal of American Chemical Society 126 (2004) 16879–16889.

[27] D.L.A. de Faria, S.V. Silva, M.T. de Oliveria, Raman microspectroscopy of some iron oxides and oxyhydroxides, Journal of Raman Spectroscopy 28 (1997) 873–878.

[28] R. Tannenbaum, M. Zubris, E.P. Goldberg, S. Reich, N. Dan, Polymer-directed nanocluster synthesis: control of particle size and morphology, Macromolecules 38 (2005) 4254–4259.

[29] T.Y. Liu, S.Y. Chen, J.H. Li, D.M. Liu, Study on drug release behaviour of CDHA/chitosan nanocomposites—Effect of CDHA nanoparticles, Journal of Controlled Release 112 (2006) 88–95.

[30] H. Lu, S. Nutt, Restricted relaxation in polymer nanocomposites near the glass transition, Macromolecules 36 (2003) 4010–4016.

[31] J. Dai, J.J. Wang, C. Sangregorio, J. Fang, E. Carpenter, J. Tang, Magnetic coupling induced increase in the blocking temperature of γ-Fe_2O_3 nanoparticles, Journal of Applied Physics 87 (2000) 7397–7399.

[32] T.Y. Liu, S.H. Hu, T.Y. Liu, D.M. Liu, S.Y. Chen. Magnetic-sensitive behavior of intelligent ferrogels for controlled release of drug, Langmuir 22 (2006) 5974–5978.